Journal of Analytical and Applied Pyrolysis 159 (2021) 105286

Contents lists available at ScienceDirect

Journal of Analytical and Applied Pyrolysis

journal homepage: www.elsevier.com/locate/jaap

Prediction of char production from slow pyrolysis of lignocellulosic biomass using multiple nonlinear regression and artificial neural network

Ting Yan Li [a], Huan Xiang [a], Yang Yang [a], Jiawei Wang [a,*], Güray Yildiz [b]

[a] Energy and Bioproducts Research Institute (EBRI), Aston University, Birmingham, B4 7ET, UK
[b] Izmir Institute of Technology, Faculty of Engineering, Department of Energy Systems Engineering, 35430, Urla, Izmir, Turkey

ARTICLE INFO

Keywords:
Char
Lignocellulosic biomass
Slow pyrolysis
Artificial neural network
Multiple nonlinear regression

ABSTRACT

Char produced from lignocellulosic biomass via slow pyrolysis have become one of the most feasible alternatives that can partially replace the utilisation of fossil fuels for energy production. In this study, the relationship between compositions of lignocellulosic biomass, operating conditions of slow pyrolysis, and characteristics of produced char have been analysed by using multiple nonlinear regression (MnLR) and artificial neural networks (ANN). Six input variables (temperature, solid residence time, production capacity, particle size, and fixed carbon and ash content) and five responses (char yield, and fixed carbon, volatile matter, ash content, HHV of produced char) were selected. A total of 57 literature references with 393–422 datasets were used to determine the correlation and coefficient of determination (R^2) between the input variables and responses. High correlation results (>0.5) existed between pyrolysis temperature and char yield (-0.502) and volatile matter of produced char (-0.619), ash content of feedstock and fixed carbon (-0.685), ash content (0.871) and HHV (-0.571) of produced char. Whilst the quadratic model was selected for the regression model, then the model was further optimised by eliminating any terms with p-values greater than 0.05. The optimised MnLR model results showed a reasonable prediction ability of char yield (R^2 = 0.5579), fixed carbon (R^2 = 0.7763), volatile matter (R^2 = 0.5709), ash (R^2 = 0.8613), and HHV (R^2 = 0.5728). ANN model optimisation was carried out as the results showed "trainbr" training algorithm, 10 neurons in the hidden layer, and "tansig" and "purelin" transfer function in hidden and output layers, respectively. The optimised ANN models had higher accuracy than MnLR models with the R^2 greater than 0.75, including 0.785 for char yield, 0.855 for fixed carbon, 0.752 for volatile matter, 0.951 for ash and 0.784 for HHV, respectively. The trained models can be used to predict and optimise the char production from slow pyrolysis of biomass without expensive experiments.

1. Introduction

Lignocellulosic biomass such as wood, forest residue and agricultural materials can be used to produce solid, liquid and gaseous products via chemical, thermochemical, and biochemical technologies [1]. Thermochemical processes, such as gasification, pyrolysis and hydrothermal liquefaction, are the most widely used technologies for biofuel production [2]. Pyrolysis is a thermal degradation process in which biomass is degraded in an oxygen-free medium with an inert carrier gas such as nitrogen to produce biofuels. Oxygen-free medium eliminates the combustion reaction and decreases the thermal stability of biomass at high temperature. The inert carrier gas can also purge the primary pyrolysis vapours out of the reactor to minimise secondary vapour phase cracking reactions. According to the heating rate and solid/vapour residence time, pyrolysis operations can be divided into two types, fast and slow pyrolysis. When liquid production is the focus, fast pyrolysis is typically applied with short solid/vapour residence times in the order of seconds (e.g. 1−2 s) and rapid heating rates (e.g. 500 W/m^2 K). If the solid product (i.e. char) is the main aim, slow pyrolysis with longer solid/-vapour residence times is preferred [3].

Slow pyrolysis operates at lower temperatures (300 °C–600 °C) along with lower heating (5−20 °C/s) and longer solid residence times (10–60 min s). Such process parameters allow the optimisation of char yield with ca. 30−50 wt% by reducing the secondary thermal cracking and volatile component releases from biomass. The char production by slow pyrolysis has been affected not only by the process parameters but also the properties of the feedstocks. As summarised by Tripathi et al. [4], reaction conditions and feedstock composition are affecting product

* Corresponding author at: Senior Lecturer in Chemical Engineering, Energy and Bioproducts Research Institute, Aston University, Birmingham, B4 7ET, UK.
E-mail address: j.wang23@aston.ac.uk (J. Wang).

https://doi.org/10.1016/j.jaap.2021.105286
Received 30 April 2021; Received in revised form 12 July 2021; Accepted 6 August 2021
Available online 10 August 2021

yield and the properties of the pyrolysis products. Critical operating conditions include pyrolysis temperature, pressure, reaction time, particle size *etc*. Increasing the pyrolysis temperature reduces the char yield as higher temperature leads to the release of the volatile components of biomass and the further thermal cracking of hydrocarbon materials. Around atmospheric pressures, in a broad range of 0.5–5 MPa, can be utilised for slow pyrolysis. Increasing the pressure will increase the gas yield, as well as the fixed carbon content and specific surface area of produced char. Long solid residence times (30–60 min s) provide sufficient time for the completion of secondary repolymerisation reactions and enhance the pore formation in char [4]. The use of inert gas can be optional, however, when utilised, the flow rate should be carefully maintained because a high flow rate will purge most of the vapour, resulting in lower vapour residence time. The preferable biomass particle size and the production capacity for slow pyrolysis are mainly dependent on the size of reactors. Usually, the biomass particle sizes in the range of 1 mm–200 mm are preferred. Increasing the biomass particle size leads to thermally thick heat transfer regimes (Biot number>>1) reducing the formed primary pyrolysis vapours that travel through the biomass layer; this results in higher repolymerisation and char formation [5]. Slow pyrolysis has been investigated via various types of reactors, including fixed-bed (batch), auger and bubbling fluidised-bed (continuous).

The compositions of the lignocellulosic biomass also have a big influence on the char production and characteristics. The physicochemical properties of the lignocellulosic biomass are measured by using proximate and ultimate analysis. Proximate includes fixed carbon (5−25 wt %), volatile matter (50−80 wt%), ash (5−20 wt%), moisture contents (10−30 wt%) and high heating value (10−30 MJ/kg), whilst ultimate includes carbon (40−60 wt%), hydrogen (5−8 wt%), oxygen (30−55 wt %), nitrogen (<1 wt%), and sulphur (<1 wt%) contents. Biomass may undergo various pre-treatment steps, such as torrefaction and solar drying, to reduce its moisture content to less than 10 wt% [6]. After slow pyrolysis, the fixed carbon content (50−80 wt%), elemental carbon content (50−80 wt%), ash content (10−50 wt%), and high heating value (15−35 wt%) significantly increases, while a decreasing trend in the volatile matter (10−25 wt%), moisture (<5 wt%), hydrogen (<5 wt%) and oxygen (5−30 wt%) contents can be observed. The aromaticity and stability of the char can be determined by the H/C molar ratios. Whilst the polarity and surface oxidation of the char can be determined by the O/C molar ratios. One of the challenges of slow pyrolysis is that the produced char contains high ash content (10-50 wt%), involving alkali and alkaline earth metals (AAEMs). Such high ash contents in the form of char cause slagging, fouling, and corrosion behaviours in the combustion process [7].

Modelling of biomass conversion processes is necessary for process scale-up, optimisation and control in industrial applications. Due to the complexity and heterogeneity of the physicochemical structure of the biomass, it is difficult to develop mathematical models to simulate biomass conversion processes from the first principles. Therefore, researchers have tried to apply other mathematic tools to tackle the problems, including multiple regression and artificial neural network.

Multiple nonlinear regression (MnLR) is a statistical tool to analyse the correlation between the input variables and responses. The correlation models can be achieved by using different functions of the regression, including linear, linear with two-factor interaction (2FI), quadratic and cubic models [8]. The accuracy of the correlation models can be determined by the measures, such as the mean squared error and the coefficient of determination R^2. The regression analysis has been widely used in the biomass conversion processes, such as predicting higher heating values [9], optimising hydrothermal carbonisation [10], pyrolysis [11,12], and gasification [13]. For example, Ates and Erginel found that the char yield of fast pyrolysis can be predicted by a logarithmic model of the pyrolysis temperature [11]. Figueiredo et al. also showed that the combined yield of monomeric aromatics and alkylphenolics in the pyrolysis oil were predicted accurately by a simple model based on the feedstock properties and reaction conditions [12].

Artificial neural network (ANN) is a self-learning method that can be used on many applications such as facial recognition, self-driving cars, price prediction for financial markets, and the predictions of possible outcomes for industrial processes. ANNs analyse a large number of datasets and trains themselves to recognise patterns between datasets, then predicts the nonlinear relationships and correlation between the input variables and responses. In the research area of bioenergy, ANNs have been developed to predict the thermal properties of biomass [14–16], and model biomass gasification [17–19], torrefaction [20], hydrolysis [21] and pyrolysis [3,22,23] processes. Zhu et al. developed prediction models for the yield and carbon contents of char produced by pyrolysis of lignocellulosic biomass using machine learning [3]. The input variables used in Zhu et al.'s study included properties of feedstock, such as contents of lignin, cellulose, hemicellulose and ash, elemental compositions and particle size, and pyrolysis conditions, such as heating rate, highest treatment temperature and residence time. 245 datasets of char yield and 128 datasets of carbon content in char were used for the model training. They found that pyrolysis temperature was the dominating factor in the char yield and carbon content of the product. One drawback of the research was the requirement of structural information and the elemental composition of the feedstock. Most of the research published on the pyrolysis of biomass only reported the proximate analysis results of feedstock, which had limited the dataset available for model training. The higher heating values of produced char was also not predicted but is relevant in the char production industry and energy-generating plants. Ozonoh et al. used ANN to optimise the torrefaction process of coal/biomass/waste tyre blends and predict char yield, enhancement factor and higher heating value using torrefaction temperature, torrefaction time and blend ratio [20]. It was shown that it was feasible to predict char yield and higher heating value of produced char using ANN models.

To our best knowledge, there is no model to predict the char yield and char properties from a slow pyrolysis. The study aims to model the relationships between the input variables (operating parameters and biomass compositions) of a slow pyrolysis process and responses (char yield and characteristics of the solid product) by using multiple regression and artificial neuron network models, as well as to identify the most accurate models. The trained models can be used to predict and optimise the char production from slow pyrolysis of biomass without expensive experiments.

2. Experimental data and analysis method

2.1. Data collection

The experimental results of char production from lignocellulosic biomass via slow pyrolysis were collected based on an extensive survey of the scientific literature. As summarised in Table 1, a total of 57 references were reviewed. Among them, 44 references were about batch operation and 13 references were about continuous operation. The number of data sets for solid yield, fixed carbon, volatile matter, ash content and higher heating values were 419, 422, 422, 422 and 393, respectively. The complete set of collected data can be found in Table S1 in the supplementary information.

Table 1
Summary of the number of references and datasets.

Operation mode	Number of references	Char yield	Fixed carbon	Volatile matter	Ash content	Higher heating value
Batch	44	350	349	349	349	340
Continuous	13	69	73	73	73	53
Total	57	419	422	422	422	393

2.2. Input variables and responses

In slow pyrolysis, various factors are affecting the product yields and their chemical/physical properties. Based on the literature investigation, seven variables were selected as the input variables, which were divided into two categories: operation parameters, involving pyrolysis temperature (°C), residence time (min), and production capacity (g), and feedstock properties, such as the particle size (mm), fixed carbon (wt% dry basis (db)) and ash content (wt% db)). The production capacity was the amount of biomass processed per batch for batch operations and the feeding rate of biomass (in g/hr) for continuous operations. Heating rate and carries gas flow rate were not selected as input variables because more than 30 % of the selected references didn't report these information. The volatile matter content of feedstock was not selected as it is dependent on the feedstock's fixed carbon and ash contents. In the case of a range of particle size of the feedstock was reported in a certain article, a mean value was calculated and taken as the reference data. The selected responses included char yield (wt% db), fixed carbon (wt% db), volatile matter (wt% db), ash content (wt% db), and HHV (MJ kg^{-1}) of the produced char. When no HHV but the elemental compositions were reported, the unified linear correlation (Eq.1) [24] was used to calculate the product's HHV. The summary of the datasets is shown in Table 2, including the number of data points, minimum, maximum, mean, and standard deviation values of each variable.

$$HHV\ (\text{MJ Kg}^{-1}) = 0.3491C + 1.1783H + 0.1005S - 0.1034O - 0.0151N - 0.0211A \quad (1)$$

Where C, H, S, O, N, and A are representing carbon (wt%), hydrogen (wt %), sulphur (wt%), oxygen (wt%), nitrogen (wt%) and ash content (wt% db), respectively.

The histograms of the input variables and responses are shown in Figs. 1 and 2. The shape of the histograms indicated the most widely used operating conditions and their distributions of the literature experiments. The histograms showed that most experiments were conducted at pyrolysis temperatures of ca. 500 °C, solid residence times of ca. 60 min, production capacities of ca. 50 g, and particle sizes of ca. 3 mm. It also indicated that most experiments were on an experimental scale as small production capacity was conducted. On the other hand, the histograms of the biomass compositions were only indicated the distributions from the literature studies as biomass was depended on the type of the biomass, its harvest time, and pre-treatment process. For example, algal biomass usually contained less than 10 wt% db of fixed carbon, but the fixed carbon of hazelnut shell could be between 13.4–27.6 wt% db, which was mainly dependent on its harvest time. Whilst the produced char's characteristics were depended on both operating conditions and composition of biomass, Fig. 2a–e showed the distribution and the highest counts of char yield (25−35 wt% db), fixed carbon (60−80 wt% db), volatile matter (5−20 wt% db), ash (0−5 wt% db), and HHV (27.5–28.5 MJ/kg).

2.3. Regression analysis

The relationship between the input variables and the responses was evaluated by multiple regressions using the software Design Expert 12. The lack-of-fit tests and model summary statistics for linear, linear with two-factor interaction (2FI), quadratic and cubic models were investigated to choose the most suitable model. The selection criterion included model p-value, lack-of-fit p-value, adjusted coefficient of determination (R^2) and predicted R^2. The general form of the models is shown in Eq. 2–Eq.5 for linear, 2FI, quadratic and cubic models, respectively.

$$y = a_0 + \sum_{1}^{k} a_i x_i + e \quad (2)$$

$$y = a_0 + \sum_{i=1}^{k} a_i x_i + \sum_{i=1}^{k} \sum_{j}^{k} a_{ij(i<j)} x_i x_j + e \quad (3)$$

$$y = a_0 + \sum_{i=1}^{k} a_i x_i + \sum_{i=1}^{k} \sum_{j}^{k} a_{ij(i<j)} x_i x_j + \sum_{i=1}^{k} a_{ii} x_i^{\ 2} + e \quad (4)$$

$$y = a_0 + \sum_{i=1}^{k} a_i x_i + \sum_{i=1}^{k} \sum_{j}^{k} a_{ij(i<j)} x_i x_j + \sum_{i=1}^{k} a_{ii} x_i^{\ 2} + \sum_{i=1}^{k} \sum_{j}^{k} \sum_{l}^{k} a_{ijl} x_i x_j x_l + e \quad (5)$$

In the models, x_1, x_2, and x_k are terms for the input variables, a_i, a_{ij}, a_{ii}, a_{ijl} are the coefficients of each term, and e is the residual of the models. For the input variables, Production capacity and Particle size, a logarithmic transformation of the raw data was carried out as the data for these two input variables covered large range. For the rest input variables, raw data was used in the regression analysis. The analysis of variance (ANOVA) for selected models was studied to obtain the mathematical relationship between the input variables and the responses. The significance of variables in the model was corrected based on p-values less than 0.05. To simplify the models, the automatic model selection feature in Design Expert was used to remove any terms with p-values greater than 0.05.

2.4. Artificial neural network model

An artificial neural network (ANN) is a mathematical model which analyses a large number of datasets and trains itself to recognise patterns between datasets. It then predicts the nonlinear relationships and correlation between the input data and responses. As shown in Fig. 3, an ANN structure consists of three layers, input, hidden and output layers. The hidden layer contains several neurons connected to the input and target parameters by adjustable weighted linkages, and the transfer

Table 2
Descriptive statistics of input variable and responses.

Variables		Unit	Count	Min	Max	Mean	Std. dev.
Input	Temperature	°C	448	300	800	515.3	125.3
	Residence time	min	448	1	180	34.2	29.4
	Production capacity	g	448	1	30,000	950.6	3935.1
	Particle size	mm	448	0.15	200	9.8	21.4
	Fixed carbon	wt% (db)	448	0	27.8	15.	5.2
	Ash	wt% (db)	448	0.2	38	6	5.8
Response	Char yield	wt% (db)	419	11.2	59	32.5	8.5
	Fixed carbon	wt% (db)	422	2.01	95.36	62.5	18.2
	Volatile matter	wt% (db)	422	1.29	66.3	21.4	12.7
	Ash	wt% (db)	422	0.6	67.7	15.1	13.8
	HHV	MJ kg^{-1} (db)	393	6.47	39.9	26.3	5.5

*db = dry basis.

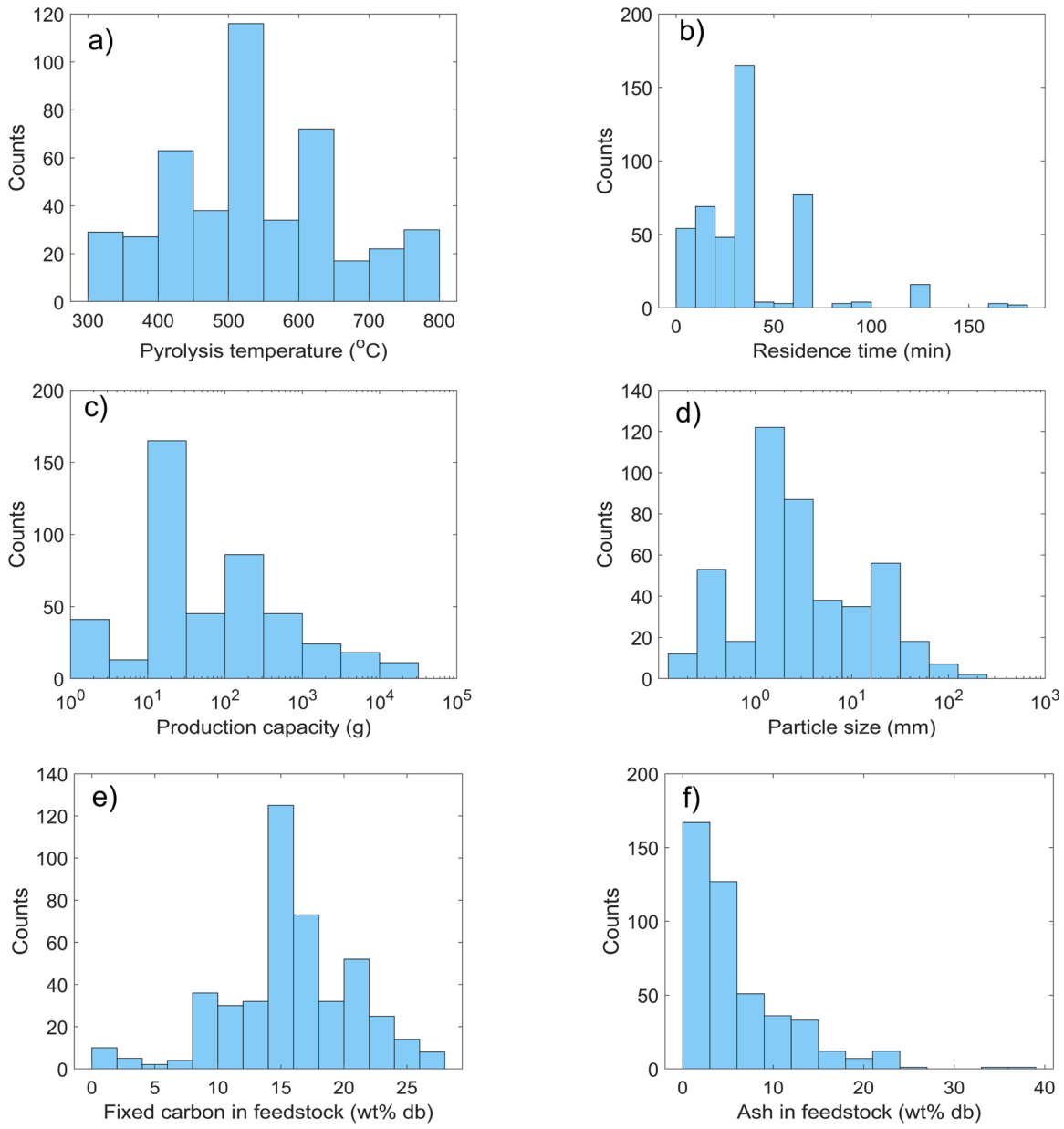

Fig. 1. Histograms of the input variables. (a) pyrolysis temperature, (b) solid residence time, (c) production capacity, (d) particle size, (e) fixed carbon of feedstock, (f). ash of feedstock.

function in the hidden layer introduces the nonlinearity to the network.

In this study, MATLAB was used to develop the ANN models to determine the relationship between the input variables and the responses. To build successful ANN models, the architectures of the ANN model had to be optimised, including the training algorithms, number of neurons, and transfer functions. The experimental datasets from the literature search were randomly divided into training, validation and testing. In the training phase, 70 % of the datasets were used, whilst the validation and testing phase used 15 % each. Large datasets for the training phase allowed the ANN model to be trained and recognised. The validation phase determined the reliability of the model, and the testing phase evaluated the outcome of the model. The input datasets were normalised into a specified range between -1 to 1 before incorporating into the network training to avoid numerical overflow due to excessively huge or small weights (Eq. 6):

$$N_p = 2\frac{(A_p - minA_p)}{(maxA_p - minA_p)} - 1 \quad (6)$$

Where N_p is the normalised parameter, A_p is the actual parameter, $minA_p$ is the minimum value of the actual parameter and $maxA_p$ is the maximum value of the actual parameter. Whilst the response datasets were unchanged to predict the actual results from the model.

In MATLAB, twelve different training algorithms are available, including Levenberg-Marquardt ("trainlm"), Bayesian Regularization ("trainbr"), BFGS Quasi-newton ("trainbfg"), Resilient Backpropagation ("trainrp")), Scaled Conjugate Gradient ("trainscg"), Conjugate Gradient with Powell/Beale Restarts ("traincgb"), Fletcher-Powell Conjugate Gradient ("traincgf"), Polak-Ribiere Conjugate Gradient ("traincgp"), One Step Secant ("trainoss"), Variable Learning Rate Gradient Descent ("traingdx"), Gradient Descent with Momentum ("traindm"), and Gradient Descent ("traingd"). MATLAB codes were developed to determine which algorithm was the best for the model in terms of their R^2 and low MSE values. During the optimisation of the training algorithms, the other parameters were kept constant, including 5 as the number of neurons in the hidden layer, tangent sigmoid ("tansig") function as the

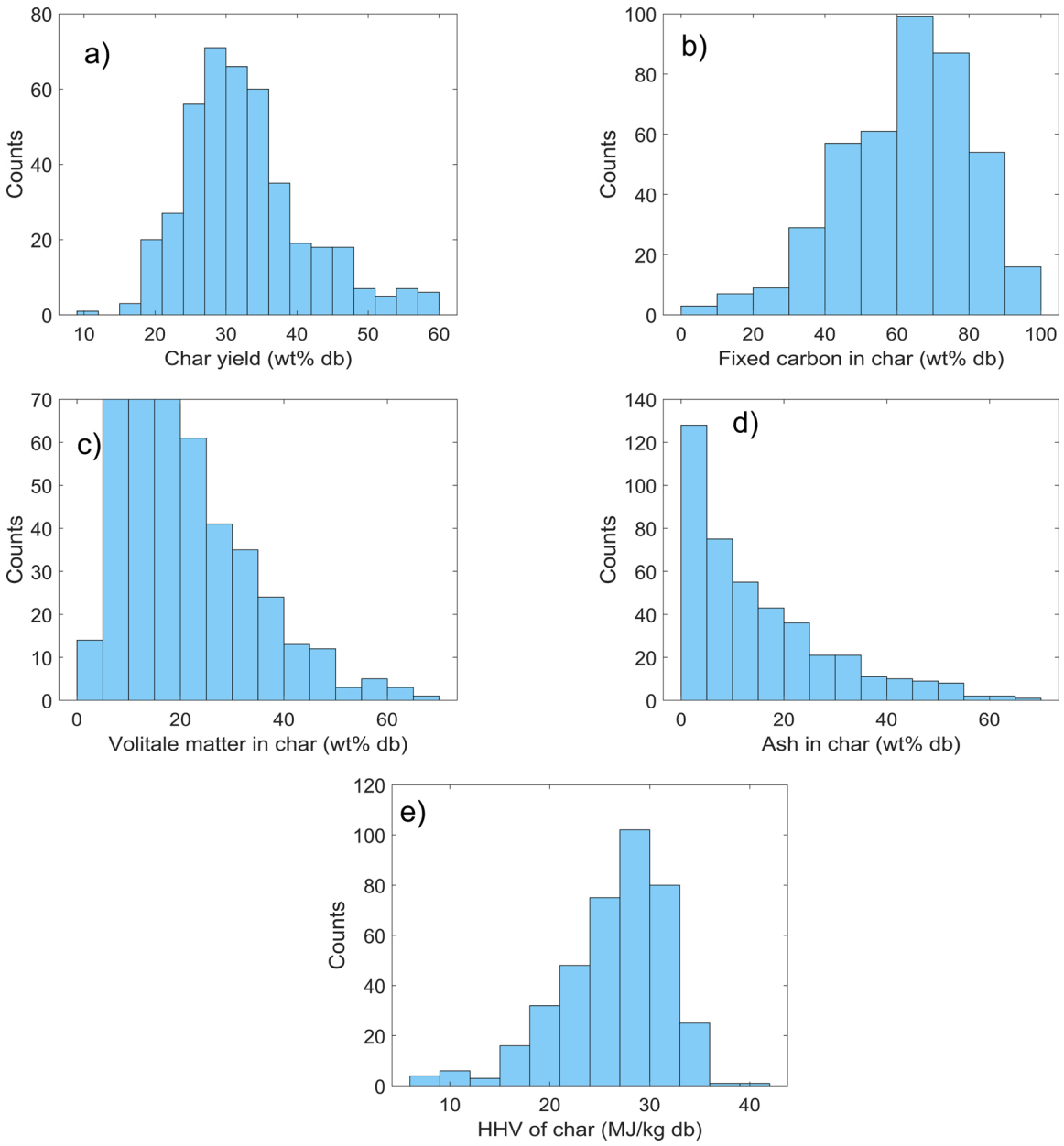

Fig. 2. Histograms of the responses. (a) char yield (wt%), (b) fixed carbon (wt%) in char, (c) volatile matter (wt%) in char, (d) ash content in char (%), (e) HHV of char.

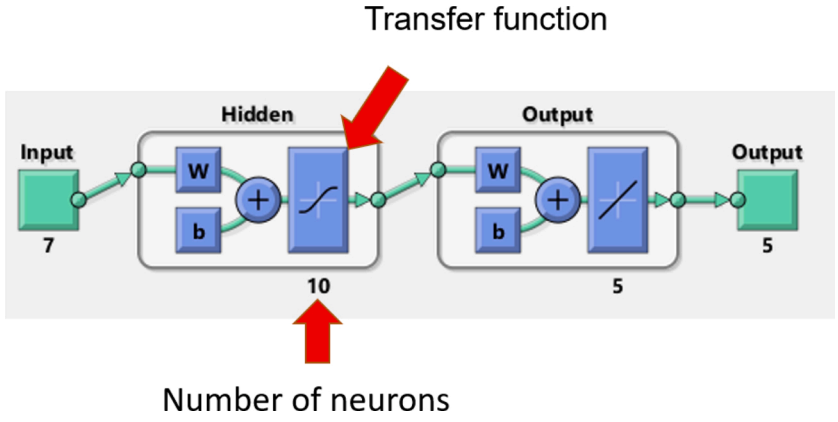

Fig. 3. The architecture of an artificial neural network.

transfer function and HHV as the response.

After the most suitable training algorithm was determined, the number of neurons in the hidden layer was needed to decide. The numbers of hidden neurons in the hidden layer are needed to determine. If the numbers of hidden neurons selected are too less as compared with the complexity of the problem, underfitting might occur where the neurons are unable to detect signals on a complicated date. If excessive hidden neurons are used, overfitting will take place, and the generalisation capability will be degraded. The number of neurons in 1–15 were evaluated for R^2 and MSE values. Same as the optimisation of the training algorithms, the other parameters were kept constant, including Bayesian Regularization ("trainbr") as the training algorithm, tangent sigmoid ("tansig") function as the transfer function and HHV as the response.

The transfer function in the hidden layer was also optimised using the same principle. Fifteen transfer functions were provided in MATLAB, including competitive transfer function ("compet"), Elliot sigmoid transfer function ("elliotsig"), positive hard limit transfer function ("hardlim), symmetric hard limit transfer function, ("hardlims"), logarithmic sigmoid transfer function ("logsig"), inverse transfer function ("netinv"), positive linear transfer function ("poslin"), linear transfer function ("purelin"), radial basis transfer function ("radbas"), radial basis normalised transfer function ("radbasn"), positive saturating linear transfer function ("satlin"), symmetric saturating linear transfer function ("satlins"), soft max transfer function ("softmax"), symmetric sigmoid transfer function ("tansig"), and triangular basis transfer function ("tribas"). The most suitable transfer function was determined when Bayesian Regularization ("trainbr") was the training algorithm, 5 was the number of neurons in the hidden layer, and HHV was the response.

After the architecture of the ANN model was optimised, the same parameters were applied to develop the models for all the responses, including char yield, char's fixed carbon, volatile matter, ash content and HHV. All MATLAB codes are included in the supplementary information.

3. Results and discussion

3.1. Raw data analysis

A correlation analysis between the input variables and responses was carried out. The Pearson's correlation coefficients and the significance level (p-value) are shown in Table 3. High correlation coefficients (>0.5) existed between pyrolysis temperature and volatile matter of produced char, ash content of feedstock and fixed carbon, volatile matter of produced char, and HHV of produced char. The scatter plots of the pairs with high correlation coefficients are shown in Fig. 4. The analysis shows that the correlation coefficient of pyrolysis temperature between char yield and char's volatile matter is -0.502 and -0.619, respectively, meaning as increasing pyrolysis temperature, the char yield and the volatile matter of the char will decrease. Whilst the ash content of biomass had a significant correlation with the fixed carbon (0.685), ash content (0.871), and HHV (-0.571) of produced char, meaning higher ash content in biomass could lead to higher ash content in char but lower fixed carbon and HHV of char. Sakulkit et al. studied the characteristics of pyrolysis products from oil palm trunk biomass [25]. They showed that, with increasing pyrolysis temperature from 400 °C to 500 °C, the volatile matter of the produced char decreased from 19.26 % to 14.15 wt %. Yang et al. indicated that the fixed carbon content rapidly increased from 63.18 wt% to 79.98 wt% when temperature increased from 300 °C to 500 °C. They also showed high temperature (>500 °C) favours the decomposition of alkaline metals of biomass to produce ash which decreases the fixed-carbon content of produced char [26].

3.2. Optimisation of MnLR model

To determine the appropriate MnLR models and to represent the relationship between the input variables and responses, the R^2, adjusted R^2 and predicted R^2 values were calculated for linear, 2FI, quadratic and cubic models, as shown in Table 4. The degrees of freedom of each model, i.e. the numbers of model coefficients, are also listed in the table. As expected, increased degrees of freedom in the models, from linear to cubic, led to higher R^2 values. However, when adjusted R^2 and predicted R^2 values were evaluated, it shows that the cubic model has over-fitted the dataset and cannot predict unseen inputs because of its negative predicted R^2 values. Therefore, the quadratic model, the one with the highest adjusted R^2 and predicted R^2 values, were selected for further optimisation. The quadratic models had a degree of freedom of 27. To simplify the models, any terms with p-values greater than 0.05 were removed. After the optimisation, the predicted R^2 values were further improved, as shown in Table 4.

The optimised models are listed in Eq. 7–11 for all five responses. The actual values and the predicted values using the optimised models are plotted in Fig. 5.

$$\begin{aligned} Char\ yield = {} & 64.4973 - 0.135679 \times A - 0.00549408 \times B + 0.463384 \\ & \times C - 8.50056 \times D + 0.532823 \times E + 1.16931 \times F \\ & + 0.0103204 \times A \times C + 0.060061 \times B \times C \\ & - 0.00924671 \times B \times E - 0.315338 \times C \times F + 0.491981 \\ & \times D \times E + 7.62325 \times 10^{-5} \times A^2 - 1.21077 \times C^2 \end{aligned} \quad (7)$$

$$\begin{aligned} FC = {} & 12.8171 + 0.174061 \times A + 0.0972342 \times B + 7.05841 \times C \\ & - 2.39589 \times D + 0.0192259 * E - 4.17954 \times F \\ & + 0.000630967 \times A \times B - 0.0201853 \times A \times C + 0.0226548 \\ & \times A \times D - 0.00267746 \times A \times F + 0.0584058 \times B \times D \\ & - 0.0135689 \times B \times E + 0.0157766 \times B \times F + 0.414499 \times C \\ & \times E - 0.651785 \times D \times E + 0.431926 \times D \times F + 0.0732588 \\ & \times E \times F - 9.20812 \times 10^{(-5)} \times A^2 - 0.00203088 \times B^2 \\ & - 1.72217 \times C^2 + 0.0811854 \times F^2 \end{aligned} \quad (8)$$

Table 3
Pearson's correlation coefficients between the input parameters and the responses. Significance between the parameters is indicated by * $p < 0.05$, ** $p < 0.01$, *** $P < 0.001$. ns indicates no significant correlation ($p > 0.05$). High correlation coefficients (<-0.5 or >0.5 are in bold).

Response					
Input variable	Char yield	Fixed carbon	Volatile matter	Ash content	HHV
Pyrolysis temperature	**−0.5023*****	0.3901***	**−0.6187*****	0.0541^{ns}	0.1208**
Residence time	−0.0597^{ns}	0.1434***	−0.1873***	−0.0127^{ns}	−0.0962^{ns}
Production capacity	−0.0185^{ns}	0.0400^{ns}	0.1193*	−0.1534**	0.0864^{ns}
Particle size	−0.0720^{ns}	0.0559^{ns}	−0.0657^{ns}	−0.0376^{ns}	0.0610^{ns}
Fixed carbon	0.0565 ^{ns}	0.4084***	−0.1155**	−0.3968***	0.4525***
Ash content	0.3884***	**−0.6850*****	0.0409^{ns}	**0.8706*****	**−0.5710*****

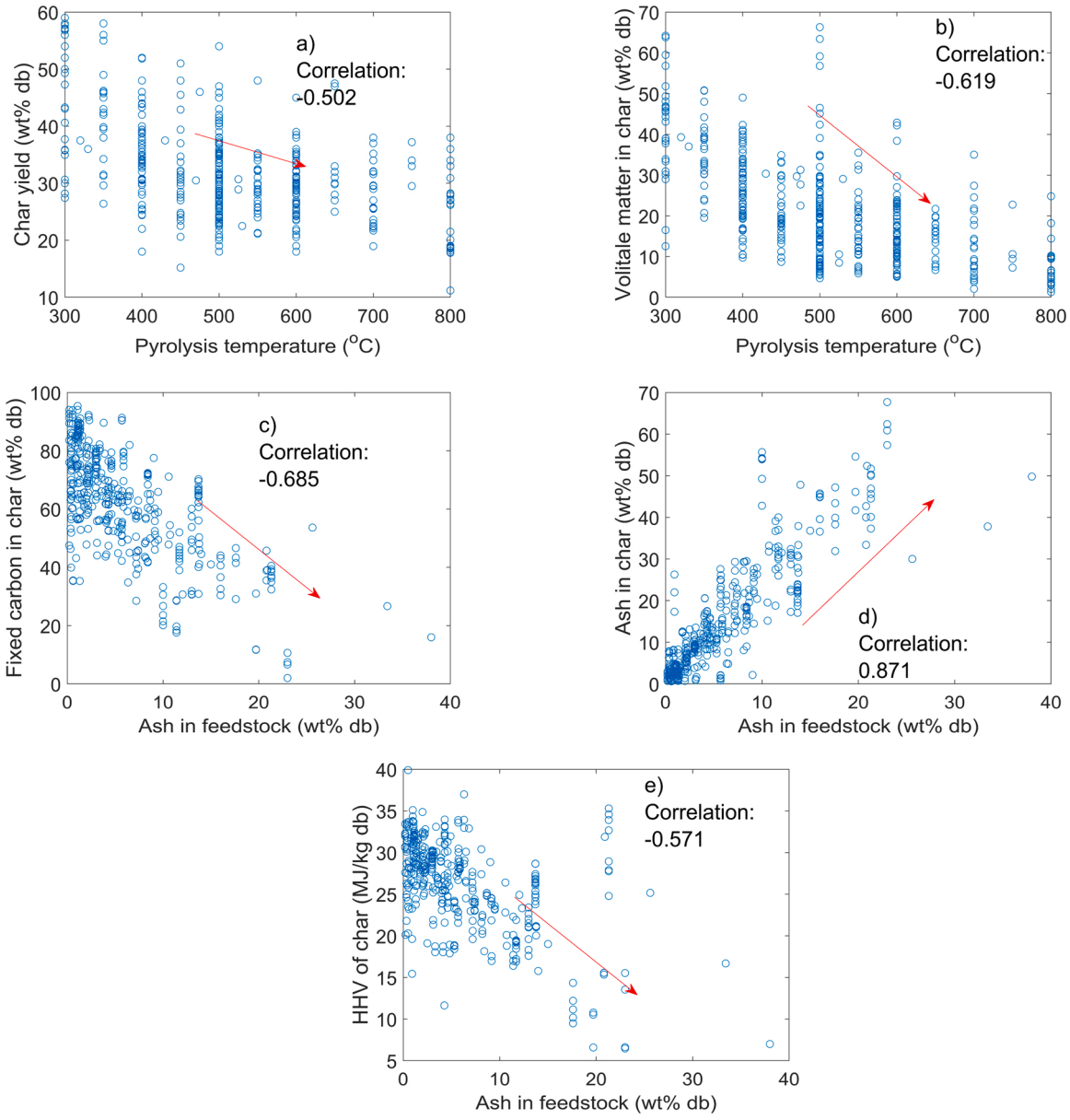

Fig. 4. Scatter plots of the pairs of input variables and responses with high correlation coefficients (>0.5). (a) char yield vs pyrolysis temperature, (b) char's volatile matter vs pyrolysis temperature, (c) char's fixed carbon vs feedstock's ash content, (d) char's ash content vs feedstock's ash content, (e) char's HHV vs feedstock's ash content.

$$VM = 94.1817 - 0.210606 \times A - 0.0806182 \times B - 5.06399 \times C + 5.05081 \times D + 0.480784 \times F - 0.858883 \times D \times F + 0.000137518 \times A^2 + 1.51123 \times C^2 \quad (9)$$

$$Ash = -13.3307 + 0.0644936 \times A + 0.013061 \times B - 2.77813 \times C - 1.2763 \times D - 0.323806 \times E + 2.79003 \times F - 0.000204887 \times A \times B + 0.00125605 \times A \times F - 0.0533454 \times B \times D - 0.0115856 \times B \times F + 0.21633 \times C \times E + 0.30372 \times C \times F - 0.0263193 \times E \times F - 5.07695 \times 10^{-5} \times A^2 + 0.00143485 \times B^2 - 0.0518208 \times F^2 \quad (10)$$

$$HHV = 19.5416 - 0.000701126 \times A + 0.0367686 \times B - 0.191607 \times C - 2.47057 \times D + 1.23483 \times E - 1.186 \times F + 9.82155 \times 10^{-5} \times A \times B + 0.00748975 \times A \times D - 0.045769 \times B \times C + 0.253446 \times C \times F - 0.0332786 \times E^2 + 0.0198405 \times F^2 \quad (11)$$

Where A, B, C, D, E and F are pyrolysis temperature (°C), residence time (min), the common logarithm of production capacity (g), the common logarithm of feedstock particle size (mm), fixed carbon (wt% db), and ash content (wt% db), respectively. The MnLR models showed poor performance for predicting char yield, volatile matter and HHV with low R2 values. It indicates that further improvement is required for accurate predictions.

Table 4
Model Summary Statistics of MnLR model.

Response						
Model		Char Yield	Fixed carbon	Volatile matter	Ash	HHV
Linear	DoF	6	6	6	6	6
	R^2	0.4310	0.6467	0.4256	0.7818	0.4288
	Adjusted R^2	0.4227	0.6416	0.4173	0.7787	0.4199
	Predicted R^2	0.4088	0.6317	0.4038	0.7705	0.4015
2FI	DoF	21	21	21	21	21
	R^2	0.5319	0.7156	05,598	0.8233	0.5223
	Adjusted R^2	0.5072	0.7007	0.5367	0.8140	0.4953
	Predicted R^2	0.4728	0.6564	0.4931	0.7795	0.4178
Quadratic	DoF	27	27	27	27	27
	R^2	0.5746	0.7783	0.6242	0.8640	0.5926
	Adjusted R^2	0.5452	0.7631	0.5984	0.8547	0.5625
	Predicted R^2	0.5048	0.7356	0.5500	0.8355	0.4989
Cubic	DoF	82	82	82	82	82
	R^2	0.7299	0.8597	0.7582	0.9223	0.7888
	Adjusted R^2	0.6639	0.8258	0.6997	0.9035	0.7330
	Predicted R^2	−0.1017	0.6490	−0.8481	0.5979	−0.0664
Optimised	DoF	13	21	8	16	12
	R^2	0.5579	0.7763	0.5709	0.8613	0.5728
	Adjusted R^2	0.5437	0.7646	0.5626	0.8558	0.5594
	Predicted R^2	0.5256	0.7444	0.5486	0.8420	0.5344

3.3. Optimisation of ANN model

As summarised in Table 5, twelve training algorithms and their analysis results including the number of iterations, mean square error (MSE) and R^2 values of training, validation, testing and overall are shown. A model with the lowest overall MSE and highest overall R^2 value is considered the best algorithm. Among all the training algorithms from Table 5, "trainbr" had the lowest MSE overall of 8.4 and highest R^2 overall of 0.703. Whilst "traincgp" was the second-best algorithm with MSE overall of 10.3 and R^2 overall of 0.657. A few literatures of using "trainbr" algorithms for ANN model have been reviewed. Nasrudin et al. found "trainbr" was the best algorithm among eleven training algorithms in modelling microwave pyrolysis of biomass [27]. It indicated the "trainbr" algorithm exhibits the best performance in predicting the weight of output and the accuracy between actual and predicted output. Serrano et al. used "trainbr" for modelling gasification in fluidised bed [28]. It showed "trainbr" achieved the highest R^2 of 0.94 for gas yield. On the other hand, fewer literatures have been proposed "trainlm" and "trainbfg" were alternative algorithms. Antwi et al. compared "trainbfg" with other ten algorithms for estimation of biogas and methane yields [29]. It showed the "trainbfg" and "traincgp" were the best algorithms among eleven training algorithms with R^2 of 0.987 and 0.979 for biogas and methane yield, respectively. Sun et al. suggested "trainlm" has an excellent performance in the prediction of pyrolysis products from industrial waste biomass [23]. It discussed "trainlm" algorithm combining with sigmoid transfer function minimised the MSE value and optimal the ANN model. Demuth et al. explained "trainbr" algorithm randomise with specified distribution variables for the weights and biases of the ANN network, then using statistical techniques to estimate the results [30]. It showed "trainbr" provides better estimation on multivariable models due to regularisation quality and early stopping of "trainbr" can ensure network to tolerate large iteration to reach its convergence. It also suggested "trainbr" works best when the dataset is normalised between -1 to 1. Therefore, "trainbr" algorithm was selected, and used as constant model variable for determine the optimum number of neurons and transfer function for this ANN model.

As summarised in Table 6, the number of neurons ranged from 1–15. Their analysis results, including the number of iterations, mean square error (MSE) and R^2 values of training, validation, testing and overall are shown. The optimum number of neurons for the model was determined by the lowest overall MSE and highest overall R^2 value. Ten neurons in the hidden layer were the most suitable for the model, with the lowest MSE overall of 6.6 and the highest R^2 overall of 0.781. Whilst nine neurons in the hidden layer were the second suitable for the model with an MSE overall of 6.8 and R^2 overall of 0.773. Decreasing the number of neurons in the hidden layer resulted in higher MSE and lower R^2 values. On the other hand, increasing the number of neurons in the hidden layer, the MSE and R^2 overall values were very close to five neurons, but the R^2 value of testing was reduced. Cheng et al. discussed the optimum number of hidden neurons was not determined by any formulae; it was determined by the MSE from different nodes within the range [31]. Therefore, ten neurons in the hidden layer were selected and were used as a constant model variable to determine the optimum training algorithm and transfer function for this ANN model.

As summarised in Table 7, fifteen transfer functions and their analysis results including number of iterations, mean square error (MSE) and R^2 values of training, validation, testing and overall are shown. Among all the transfer function in Table 7, "tansig" was the best transfer function for the model with the lowest MSE overall of 6.7 and the highest R^2 overall of 0.776. Whilst "elliotsig" had the MSE overall of 8.1 and R^2 overall of 0.731. In this model, "tansig" transfer function was used in the hidden layer, and "purelin" was used in the output layer. Cakman et al. discussed the "tansig" in the first hidden layer and "purelin" in the second hidden layer increased the ability of the ANN model to determine for both linear and nonlinear relationships between the input on the target variables [32]. Zhong et al. compared six different activation function sets in modelling fast pyrolysis via fluidised-bed and found "tansig" function was suitable for both hidden and output layer [33]. Therefore, "tansig" function was selected in the hidden layer, and "purelin" was selected in the output layer.

As summarised in Table 8, the response variables and their analysis results from ANN models including number of iterations, mean square error (MSE) and R^2 values of training, validation, testing and overall are shown. The plots of the ANN training, validation and test can be found in the supplementary information as Figure S1-S5. The optimised model variables were used to obtain the results of the responses, including "trainbr" as training algorithm, ten neurons in a hidden layer, and "tansig" and "purelin" transfer function in hidden and output layers, respectively. To ensure the reliability of the R^2 overall value, all the R^2 values of training, validation, and testing were achieved with less than maximum of 0.1 different between the values. The results showed that high R^2 values were obtained for all response variables, including char yield (0.785), fixed carbon (0.855), volatile matter (0.752), ash (0.951), and HHV (0.784). The actual values and the predicted values using the ANN models are plotted in Fig. 6. The ANN models in the MATLAB script

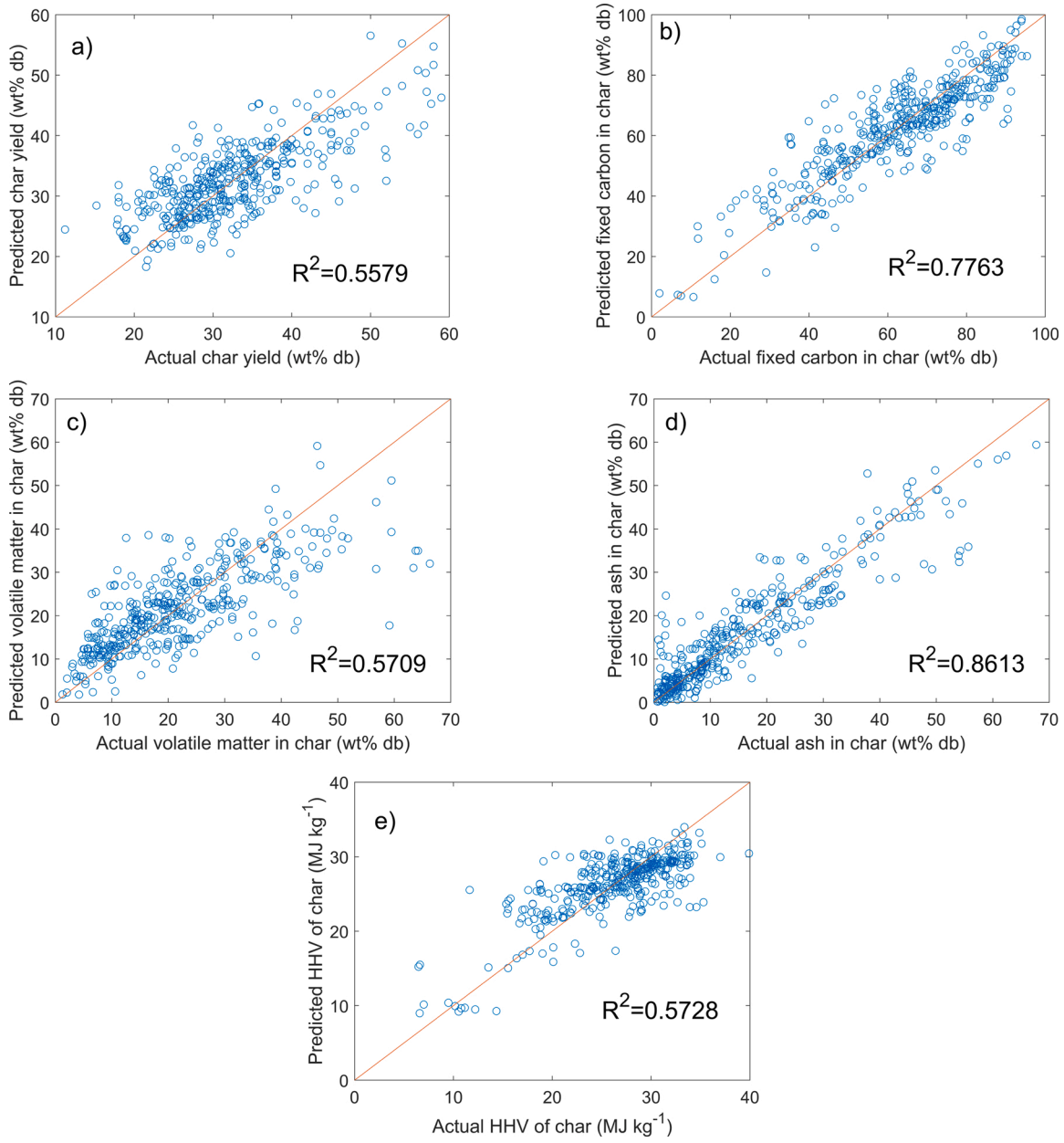

Fig. 5. Plots of the actual and predicted values obtained from the regression model: (a) char yield (wt%), (b) fixed carbon in char (wt% db), (c) volatile matter in char (wt% db), (d) ash content in char (wt% db) and (e) HHV of char (MJ kg^{-1}).

Table 5
Summary of training algorithm statistic (Tr: training, V: validation, T: test, O: overall).

Training algorithm	Number of iterations	Mean square error (MSE)				R^2			
		Tr	V	T	O	Tr	V	T	O
trainlm	63	10.9	13.3	11.3	11.3	0.638	0.630	0.569	0.624
trainbr	**117**	**8.4**	**12.1**	**8.4**	**8.9**	**0.730**	**0.593**	**0.706**	**0.703**
trainbfg	112	9.3	11.9	19.5	11.2	0.708	0.521	0.369	0.630
trainrp	68	18.1	16.8	11.8	17.0	0.407	0.494	0.563	0.439
trainscg	160	14.2	18.0	16.7	15.2	0.517	0.437	0.460	0.494
traincgb	67	16.9	17.4	19.0	17.3	0.421	0.422	0.441	0.422
traincgf	76	14.8	12.4	15.9	14.6	0.528	0.425	0.497	0.512
traincgp	196	9.1	13.2	12.8	10.3	0.717	0.443	0.534	0.657
trainoss	113	13.4	19.1	16.4	14.7	0.563	0.410	0.401	0.510
traingdx	394	13.5	16.9	16.0	14.4	0.537	0.516	0.455	0.520
traingdm	154	30.2	26.5	35.1	30.4	0.012	0.002	0.166	0.032
traingd	50	1144.4	1201.2	1056.5	1139.7	0.013	0.035	0.081	0.024

Table 6
Summary of the number of neurons statistic (Tr: training, V: validation, T: test, O: overall).

Number of neurons	Number of iterations	Mean square error (MSE)				R^2			
		Tr	V	T	O	Tr	V	T	O
1	57	16.1	16.9	21.5	17.0	0.450	0.307	0.461	0.433
2	62	14.3	14.1	17.7	14.8	0.541	0.587	0.224	0.507
3	67	11.4	13.2	19.6	12.9	0.650	0.505	0.221	0.573
4	74	8.3	10.8	17.2	10.0	0.722	0.609	0.519	0.665
5	67	9.6	11.6	11.4	10.2	0.662	0.611	0.710	0.662
6	77	8.2	10.9	9.9	8.9	0.719	0.668	0.710	0.705
7	53	15.5	18.6	14.2	15.7	0.511	0.425	0.489	0.493
8	81	7.3	14.4	9.1	8.6	0.757	0.596	0.643	0.712
9	110	6.0	6.3	11.0	6.8	0.815	0.790	0.430	0.773
10	**108**	**4.6**	**14.9**	**7.4**	**6.6**	**0.829**	**0.623**	**0.788**	**0.781**
11	76	9.0	12.2	25.5	12.0	0.689	0.613	0.328	0.601
12	72	7.0	11.6	10.6	8.2	0.797	0.449	0.562	0.730
13	111	4.7	6.8	23.5	7.9	0.849	0.750	0.416	0.746
14	99	6.8	10.8	5.4	7.2	0.781	0.610	0.823	0.761
15	80	7.1	10.5	16.4	9.0	0.741	0.787	0.475	0.701

Table 7
Summary of transfer functions statistic (Tr: training, V: validation, T: test, O: overall).

Transfer functions	Number of iterations	Mean square error (MSE)				R^2			
		Tr	V	T	O	Tr	V	T	O
compet	11	25.7	33.4	40.1	29.0	0.056	0.008	0.018	0.037
elliotsig	130	6.7	12.4	10.3	8.1	0.789	0.571	0.638	0.731
hardlim	78	22.4	18.4	29.9	22.9	0.278	0.201	0.209	0.253
hardlims	80	20.7	12.2	28.2	20.5	0.270	0.364	0.443	0.315
logsig	75	8.1	7.8	17.1	9.4	0.740	0.714	0.464	0.689
netinv	81	13.4	15.4	58.1	20.4	0.574	0.586	0.000	0.370
poslin	64	12.4	12.4	15.9	12.9	0.611	0.537	0.437	0.571
purelin	1000	17.4	17.5	23.7	18.4	0.412	0.488	0.411	0.426
radbas	124	4.4	11.8	27.8	9.0	0.852	0.652	0.199	0.700
radbasn	60	9.9	15.5	15.5	11.6	0.633	0.650	0.535	0.616
satlin	60	13.1	7.6	12.5	12.2	0.594	0.664	0.551	0.594
satlins	35	15.4	14.8	16.6	15.5	0.520	0.163	0.501	0.484
softmax	72	8.8	11.0	10.5	9.4	0.748	0.509	0.478	0.687
tansig	**95**	**5.7**	**9.3**	**8.7**	**6.7**	**0.802**	**0.735**	**0.717**	**0.776**
tribas	122	10.7	12.5	11.4	11.1	0.648	0.630	0.561	0.632

Table 8
Summary of responses statistic of ANN model (Tr: training, V: validation, T: test, O: overall).

Response	Number of iterations	Mean square error (MSE)				R^2			
		Tr	V	T	O	Tr	V	T	O
Char yield	194	12.8	25.8	17.5	15.500	0.830	0.612	0.743	0.785
Fixed carbon	128	42.3	58.8	64.3	48.1	0.879	0.782	0.809	0.855
Volatile matter	123	37.1	49.3	43.7	39.9	0.770	0.720	0.697	0.752
Ash	144	5.0	20.2	18.4	9.3	0.974	0.889	0.900	0.951
HHV	115	6.5	6.9	6	6.5	0.764	0.847	0.751	0.784

format are included in the supplementary information, containing all the weights and bias for the networks. The accuracy of the prediction of the char yield is close to the ones ($R^2 = 0.8462$, 0.8049 and 0.8548 for different sets of inputs) reported by Zhu et al. [3] using the random forest method.

3.4. Comparison of ANN and MnLR models

The model comparison was made by comparing the R^2 overall value of the ANN and MnLR models. The MnLR model obtained the R^2 overall values of char yield (0.5579), fixed carbon (0.7763), volatile matter (0.5709), ash (0.8613), HHV (0.5728) shown in Table 4. Whilst the ANN model determined the R^2 overall values of char yield (0.785), fixed carbon (0.855), volatile matter (0.752), ash (0.951), and HHV (0.784) shown in Table 8. The results showed that all the response variables from the ANN model had higher R^2 overall values than MnLR models. It can be concluded that ANN model has a higher ability to analyse and evaluate the datasets to achieve better results. Although the MnLR models had lower R^2 values than ANN models, it indicated a similar relationship as ANN model, including ash had the highest R^2 overall value among all the response variables, whilst fixed carbon had the second-highest R^2 overall value. Some literature reviews that compared regression and ANN models were reviewed. Tosun et al. compared the linear regression and ANN models of biodiesel [34]. They showed that the ANN model with "trainlm" algorithm, "logsig" in the hidden layer and "purelin" in output layers obtained lower mean absolute percentage error (MAPE) values than linear regression. Kumar et al. also compared the linear regression and ANN models of soybean biodiesel yield [35]. It was concluded that ANN model with "trainlm" algorithm and "logsig" transfer function were more accurate than linear regression (R^2 values were 0.9899 and 0.4198, respectively). However, Mesroghli et al. showed the results of US coal's HHV estimation from ANN, and

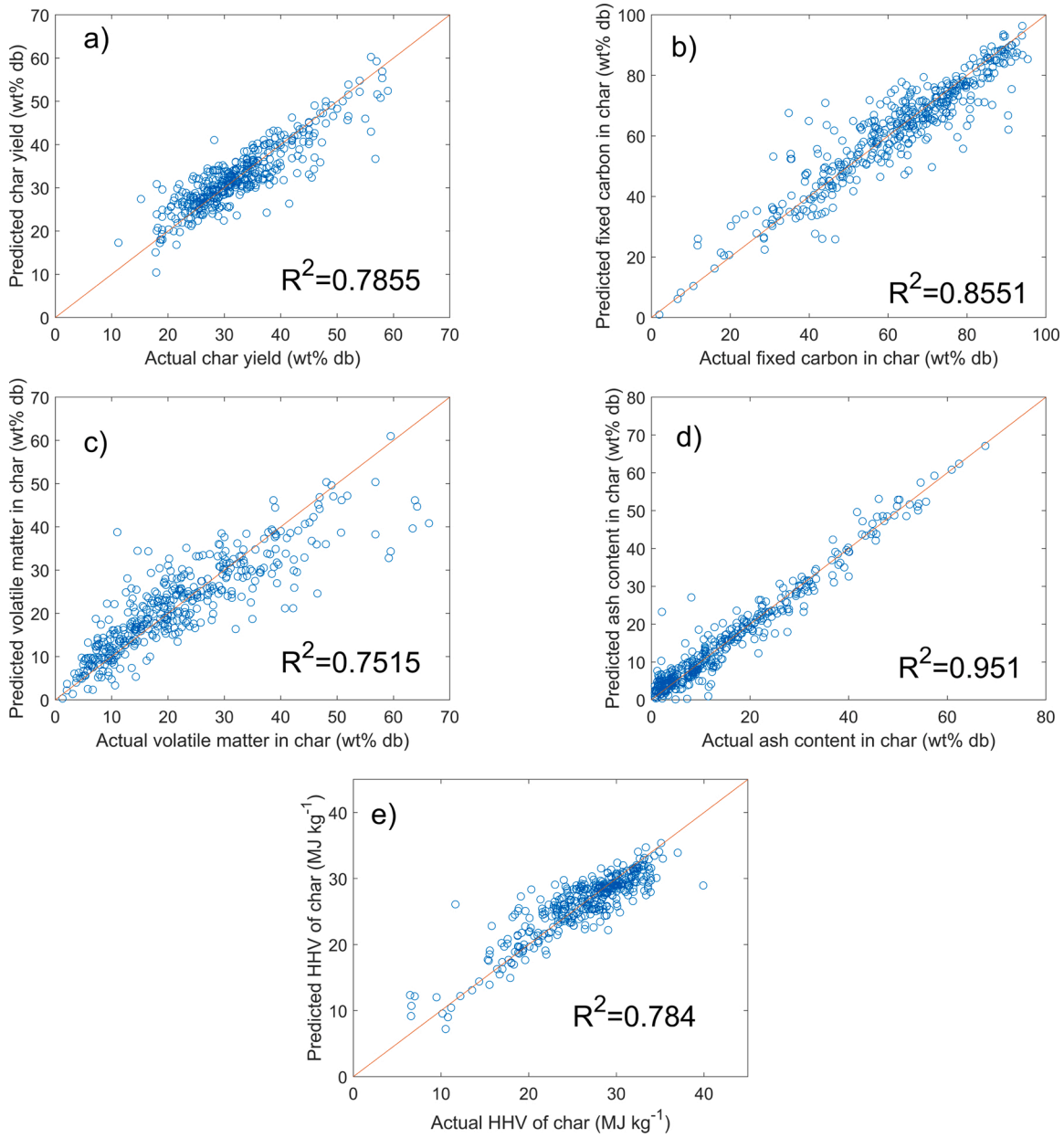

Fig. 6. Plots of the actual and predicted values obtained from ANN model: (a) char yield (wt%), (b) fixed carbon in char (wt% db), (c) volatile matter in char (wt% db), (d) ash content in char (wt% db) and (e) HHV of char (MJ kg^{-1}).

regression did not have much different [36]. They suggested that using common and understood techniques as regression was better than using a more complicated method as ANN.

4. Conclusions

In this study, the relationship between the compositions of lignocellulosic biomass and operating parameters for slow pyrolysis and produced char's characteristics were successfully carried out based on a modelling work. Six input variables, including temperature, residence time, production capacity, particle diameter, fixed carbon and ash, and five response variables including char yield, fixed carbon, volatile matter, ash, and HHV were evaluated by using an artificial neuron network (MATLAB) and multiple nonlinear regression models (Design Expert 12). A total of 422 literature datasets were searched and normalised in the range of -1 to 1 for ANN model analysation. High correlation results (>0.5) existed between pyrolysis temperature and volatile matter of produced char (-0.502), ash content of feedstock and fixed carbon (-0.619), ash content (0.871) and HHV (-0.571) of produced char were analysed by the ANN model. Model optimisation and comparison were carried in both models. The determination coefficient R^2 was used to compare the results and determine the accuracy of the models. All twelve training algorithms, neurons ranged from 1 to 15, and fifteen transfer functions were evaluated for the ANN model. The results showed the most suitable model parameters for the ANN model were "trainbr" training algorithm, ten neurons in the hidden layer, and "tansig" and "purelin" transfer functions in hidden and output layers, respectively. Then the optimised model parameters for ANN were used to determine the results of the response variables. The results showed high R^2 for all responses, including char yield ($R^2 = 0.785$), fixed carbon ($R^2 = 0.855$), volatile matter ($R^2 = 0.752$), ash ($R^2 = 0.951$), and HHV ($R^2 = 0.784$). Whilst four models were compared in the MnLR model, and it was shown that the quadratic models had the highest R^2, adjusted R^2, and predicted R^2 among all the models. The quadratic models were

further optimised by eliminating any terms with p-values greater than 0.05, and the optimised equations for MnLR were achieved. The optimised MnLR model results showed a good prediction ability of char yield (R^2 = 0.5579), fixed carbon (R^2 = 0.7763), volatile matter (R^2 = 0.5709), ash (R^2 = 0.8613), and HHV (R^2 = 0.5728). Among all the results obtained from ANN and MnLR models, it can be concluded that ANN models had higher accuracy than MnLR models in predicting the relationship between input and response variables. The models developed in the study can be used to estimate and optimise the char production and quality by slow pyrolysis of biomass.

CRediT authorship contribution statement

Ting Yan Li: Investigation, Formal analysis, Writing - original draft. **Huan Xiang:** Formal analysis, Writing - review & editing. **Yang Yang:** Supervision, Writing - review & editing, Funding acquisition. **Jiawei Wang:** Supervision, Writing - review & editing, Funding acquisition. **Güray Yildiz:** Writing - review & editing, Funding acquisition.

Declaration of Competing Interest

The authors declare that they have no known competing financial interests or personal relationships that could have appeared to influence the work reported in this paper.

Acknowledgements

The work was supported by an Institutional Links grant (No. 527641843), under the Turkey partnership. The grant is funded by the UK Department for Business, Energy and Industrial Strategy together with the Scientific and Technological Research Council of Turkey (TÜBİTAK; Project no. 119N302) and delivered by the British Council.

Appendix A. Supplementary data

Supplementary data associated with this article can be found, in the online version, at https://doi.org/10.1016/j.jaap.2021.105286.

References

[1] T. Kan, V. Strezov, T.J. Evans, Lignocellulosic biomass pyrolysis: a review of product properties and effects of pyrolysis parameters, Renewable Sustainable Energy Rev. 57 (2016) 1126–1140, https://doi.org/10.1016/j.rser.2015.12.185.
[2] C.E. Brewer, K. Schmidt-Rohr, J.A. Satrio, R.C. Brown, Characterization of biochar from fast pyrolysis and gasification systems, Environ. Prog. Sustain. Energy 28 (2009) 386–396, https://doi.org/10.1002/ep.10378.
[3] X. Zhu, Y. Li, X. Wang, Machine learning prediction of biochar yield and carbon contents in biochar based on biomass characteristics and pyrolysis conditions, Bioresour. Technol. 288 (2019) 121527, https://doi.org/10.1016/j.biortech.2019.121527.
[4] M. Tripathi, J.N. Sahu, P. Ganesan, Effect of process parameters on production of biochar from biomass waste through pyrolysis: a review, Renewable Sustainable Energy Rev. 55 (2016) 467–481, https://doi.org/10.1016/j.rser.2015.10.122.
[5] A. Demirbas, Effects of temperature and particle size on bio-char yield from pyrolysis of agricultural residues, J. Anal. Appl. Pyrolysis 72 (2004) 243–248, https://doi.org/10.1016/j.jaap.2004.07.003.
[6] W.H. Chen, J. Peng, X.T. Bi, A state-of-the-art review of biomass torrefaction, densification and applications, Renewable Sustainable Energy Rev. 44 (2015) 847–866, https://doi.org/10.1016/j.rser.2014.12.039.
[7] F. Ronsse, S. van Hecke, D. Dickinson, W. Prins, Production and characterization of slow pyrolysis biochar: influence of feedstock type and pyrolysis conditions, Gcb Bioenergy 5 (2013) 104–115, https://doi.org/10.1111/gcbb.12018.
[8] E. Siemsen, A. Roth, P. Oliveira, Common method Bias in regression models with linear, quadratic, and interaction effects, Organ. Res. Methods 13 (2010) 456–476, https://doi.org/10.1177/1094428109351241.
[9] I. Boumanchar, K. Charafeddine, Y. Chhiti, F.E. M'hamdi Alaoui, A. Sahibed-dine, F. Bentiss, C. Jama, M. Bensitel, Biomass higher heating value prediction from ultimate analysis using multiple regression and genetic programming, Biomass Convers. Biorefinery. 9 (2019) 499–509, https://doi.org/10.1007/s13399-019-00386-5.
[10] M.J. Jiménez Toro, X. Dou, I. Ajewole, J. Wang, K. Chong, N. Ai, G. Zeng, T. Chen, M.J.J. Toro, X. Dou, I. Ajewole, J. Wang, K. Chong, N. Ai, G. Zeng, T. Chen, Preparation and optimization of macroalgae-derived solid acid catalysts, Waste Biomass Valorization 10 (2019) 805–816, https://doi.org/10.1007/s12649-017-0101-0.
[11] F. Ateş, N. Erginel, The regression analysis of fast pyrolysis product yields and determination of product quality, Fuel 102 (2012) 681–690, https://doi.org/10.1016/j.fuel.2012.05.051.
[12] M.B. Figueirêdo, P.J. Deuss, R.H. Venderbosch, H.J. Heeres, Catalytic hydrotreatment of pyrolytic lignins from different sources to biobased chemicals: identification of feed-product relations, Biomass Bioenergy 134 (2020) 105484, https://doi.org/10.1016/j.biombioe.2020.105484.
[13] M. Puig-Arnavat, J.C. Bruno, A. Coronas, Review and analysis of biomass gasification models, Renewable Sustainable Energy Rev. 14 (2010) 2841–2851, https://doi.org/10.1016/j.rser.2010.07.030.
[14] H. Uzun, Z. Yıldız, J.L. Goldfarb, S. Ceylan, Improved prediction of higher heating value of biomass using an artificial neural network model based on proximate analysis, Bioresour. Technol. 234 (2017) 122–130, https://doi.org/10.1016/j.biortech.2017.03.015.
[15] J.O. Ighalo, A.G. Adeniyi, G. Marques, Application of artificial neural networks in predicting biomass higher heating value: an early appraisal, Energy Sources, Part A recover, Util. Environ. Eff. (2020), https://doi.org/10.1080/15567036.2020.1809567.
[16] O. Obafemi, A. Stephen, O. Ajayi, M. Nkosinathi, A survey of artificial neural network-based prediction models for thermal properties of biomass. Procedia Manuf., Elsevier B.V., 2019, pp. 184–191, https://doi.org/10.1016/j.promfg.2019.04.103.
[17] J. George, P. Arun, C. Muraleedharan, Assessment of producer gas composition in air gasification of biomass using artificial neural network model, Int. J. Hydrogen Energy 43 (2018) 9558–9568, https://doi.org/10.1016/j.ijhydene.2018.04.007.
[18] R. Mikulandrić, D. Lončar, D. Böhning, R. Böhme, M. Beckmann, Artificial neural network modelling approach for a biomass gasification process in fixed bed gasifiers, Energy Convers. Manage. 87 (2014) 1210–1223, https://doi.org/10.1016/j.enconman.2014.03.036.
[19] M. Puig-Arnavat, J.A. Hernández, J.C. Bruno, A. Coronas, Artificial neural network models for biomass gasification in fluidized bed gasifiers, Biomass Bioenergy 49 (2013) 279–289, https://doi.org/10.1016/j.biombioe.2012.12.012.
[20] M. Ozonoh, B.O. Oboirien, M.O. Daramola, Optimization of process variables during torrefaction of coal/biomass/waste tyre blends: application of artificial neural network & response surface methodology, Biomass Bioenergy 143 (2020) 105808, https://doi.org/10.1016/j.biombioe.2020.105808.
[21] S. Vani, R.K. Sukumaran, S. Savithri, Prediction of sugar yields during hydrolysis of lignocellulosic biomass using artificial neural network modeling, Bioresour. Technol. 188 (2015) 128–135, https://doi.org/10.1016/j.biortech.2015.01.083.
[22] S. Sunphorka, B. Chalermsinsuwan, P. Piumsomboon, Artificial neural network model for the prediction of kinetic parameters of biomass pyrolysis from its constituents, Fuel 193 (2017) 142–158, https://doi.org/10.1016/j.fuel.2016.12.046.
[23] Y. Sun, L. Liu, Q. Wang, X. Yang, X. Tu, Pyrolysis products from industrial waste biomass based on a neural network model, J. Anal. Appl. Pyrolysis 120 (2016) 94–102, https://doi.org/10.1016/j.jaap.2016.04.013.
[24] S.A. Channiwala, P.P. Parikh, A unified correlation for estimating HHV of solid, liquid and gaseous fuels, Fuel 81 (2002) 1051–1063, https://doi.org/10.1016/S0016-2361(01)00131-4.
[25] P. Sakulkit, A. Palamanit, R. Dejchanchaiwong, P. Reubroycharoen, Characteristics of pyrolysis products from pyrolysis and co-pyrolysis of rubber wood and oil palm trunk biomass for biofuel and value-added applications, J. Environ. Chem. Eng. 8 (2020) 104561, https://doi.org/10.1016/j.jece.2020.104561.
[26] X. Yang, K. Kang, L. Qiu, L. Zhao, R. Sun, Effects of carbonization conditions on the yield and fixed carbon content of biochar from pruned apple tree branches, Renew. Energy 146 (2020) 1691–1699, https://doi.org/10.1016/j.renene.2019.07.148.
[27] N.A. Nasrudin, J. Jewaratnam, M.A. Hossain, P.B. Ganeson, Performance comparison of feedforward neural network training algorithms in modelling microwave pyrolysis of oil palm fibre for hydrogen and biochar production, Asia-Pacific J. Chem. Eng. 15 (2020) e2388, https://doi.org/10.1002/apj.2388.
[28] D. Serrano, I. Golpour, S. Sánchez-Delgado, Predicting the effect of bed materials in bubbling fluidized bed gasification using artificial neural networks (ANNs) modeling approach, Fuel 266 (2020) 117021, https://doi.org/10.1016/j.fuel.2020.117021.
[29] P. Antwi, J. Li, P.O. Boadi, J. Meng, E. Shi, K. Deng, F.K. Bondinuba, Estimation of biogas and methane yields in an UASB treating potato starch processing wastewater with backpropagation artificial neural network, Bioresour. Technol. 228 (2017) 106–115, https://doi.org/10.1016/j.biortech.2016.12.045.
[30] H. Demuth, M. Beale, Neural Network Toolbox User's Guide: for Use with MATLAB, The MathWorks, Inc., 2004.
[31] J. Cheng, X. Wang, T. Si, F. Zhou, J. Zhou, K. Cen, Ignition temperature and activation energy of power coal blends predicted with back-propagation neural network models, Fuel 173 (2016) 230–238, https://doi.org/10.1016/j.fuel.2016.01.043.
[32] G. Çakman, S. Gheni, S. Ceylan, Prediction of higher heating value of biochars using proximate analysis by artificial neural network, (n.d.). https://doi.org/10.1007/s13399-021-01358-4.
[33] H. Zhong, Q. Xiong, L. Yin, J. Zhang, Y. Zhu, S. Liang, B. Niu, X. Zhang, CFD-based reduced-order modeling of fluidized-bed biomass fast pyrolysis using artificial neural network, Renew. Energy 152 (2020) 613–626, https://doi.org/10.1016/j.renene.2020.01.057.
[34] E. Tosun, K. Aydin, M. Bilgili, Comparison of linear regression and artificial neural network model of a diesel engine fueled with biodiesel-alcohol mixtures,

Alexandria Eng. J. 55 (2016) 3081–3089, https://doi.org/10.1016/j.aej.2016.08.011.

[35] S. Kumar, Comparison of linear regression and artificial neural network technique for prediction of a soybean biodiesel yield, Energy Sources, Part A recover, Util. Environ. Eff. 42 (2020) 1425–1435, https://doi.org/10.1080/15567036.2019.1604858.

[36] S. Mesroghli, E. Jorjani, S. Chehreh Chelgani, Estimation of gross calorific value based on coal analysis using regression and artificial neural networks, Int. J. Coal Geol. 79 (2009) 49–54, https://doi.org/10.1016/j.coal.2009.04.002.